Growth Dynamics and Morphology of Oleic Acid Vapor-Deposited on a Silica Surface†

Eva R. Garland,‡ Amy D. Lee,§ Tomas Baer,*,‡ and Laura I. Clarke*,§

Department of Chemistry, University of North Carolina, Chapel Hill, North Carolina 27599-3290, Department of Physics, North Carolina State University, Raleigh, North Carolina 27695-8202

Received: July 31, 2008; Revised Manuscript Received: September 22, 2008

The vapor deposition of oleic acid onto silica surfaces at 25% relative humidity and temperatures ranging from 60 to 80 °C is found to proceed in three stages: (I) rapid formation of monolayer-high islands of approximately 100 nm diameter on timescales of a few minutes; (II) relatively little growth over timescales of tens to hundreds of minutes; and (III) a linear increase in apparent thickness as a function of time, characterized by the formation of multilayer islands on time scales of thousands of minutes. The rate of growth in region III is faster at higher temperatures. This growth process is analyzed in the context of the transition from two-dimensional to three-dimensional island growth at submonolayer coverage observed for metal vapor deposition on oxide surfaces. At a relative humidity of 94%, with several layers of water molecules present on the silica surface, the oleic acid wets the surface rather than forming discrete islands.

Introduction

Airborne organic species may deposit onto surfaces ranging from aerosol particles to buildings and interior walls. These surface-bound organics impact the environment in many ways. In the case of aerosols, organic coatings may affect reactive,[1] hygroscopic,[2] and radiative properties.[3,4] Deposition of airborne organic species onto buildings and historical monuments contributes to black crusts that must be removed for aesthetic reasons as well as for the preservation of the structure; however, many cleaning methods result in damage to the underlying building materials.[5] Organic species that desorb slowly from interior walls can negatively impact indoor air quality over long periods of time.[6]

To assess the impact of adsorbed organic species on environmental surfaces, it is necessary to understand the details of the sorption process, including thermodynamic and kinetic aspects, along with film morphology. For example, the orientation of the organic species on the surface may affect subsequent reactivity and hydrophobicity of the surface.[7,8] Such orientation effects may be particularly enhanced for amphiphilic adsorbates.[9] The formation of islands of organic species on the surface, as opposed to an even coating, could allow for exposure of the underlying surface, even for quantities of the organic species that correspond to several monolayers of coverage. Thus, many of the properties of the underlying surface (catalytic ability, radiative properties, etc.) would remain intact. The surface area to volume ratio of the islands can also impact the oxidation rate of the organic species.[10]

Many studies of the morphology of organic adsorbates on inorganic surfaces have been carried out in the context of preparing thin films for the semiconductor industry.[11−14] Most work in this field has focused on tuning deposition conditions such that island formation is minimized, and many of these studies have been performed under high vacuum conditions, which are not directly applicable to environmentally motivated studies. In contrast, environmentally motivated laboratory research has utilized vapor deposition techniques to adsorb organic compounds onto surfaces as a model for the much more complex processes in the atmosphere; however the morphology of the resulting films has not generally been characterized. Our work bridges this gap by applying film characterization techniques to examine the structure of organic species that deposit onto inorganic surfaces via vapor deposition under conditions similar to those employed in atmospheric chemistry laboratory experiments as a step toward understanding real-world coating processes.

The potentially significant role of organic species coated onto atmospheric surfaces has motivated our studies of the kinetic, thermodynamic, and structural details of the adsorption of oleic acid onto silica surfaces. Oleic acid is a C-18 monounsaturated fatty acid released into the atmosphere from meat cooking and is one of many low-volatility long-chain fatty acids in the atmosphere that may deposit onto surfaces.[15] Oleic acid has a very low vapor pressure at atmospheric temperatures and therefore undergoes homogeneous nucleation or deposits onto existing aerosol particles or other surfaces (such as chimney walls) soon after being released into the atmosphere. We chose to utilize oleic acid for these studies as a model organic fatty acid molecule since it has been well-studied in the context of aerosol particles. The primary purpose of this work is to understand coating morphologies of amphiphilic molecules on oxide surfaces.

We previously have reported that a submonolayer coverage of oleic acid vapor-deposited onto silica forms islands, rather than coating the surface evenly.[16] In that study, we found that once a critical number of islands formed, the growth slowed asymptotically, and that neither multilayer formation nor a uniform monolayer was observed over a time scale of hours at 70 °C.

Here, we extend our studies on the deposition of oleic acid on silica to longer periods of time and over a broader range of deposition temperatures and relative humidities. We use ellipsometry to follow the growth kinetics, atomic force microscopy (AFM) to investigate the structure of the oleic acid mono- and

† Part of the special section "Physical Chemistry of Environmental Interfaces".

* Corresponding authors. E-mails: (T.B.) baer@email.unc.edu, (L.I.C.) Laura_Clarke@ncsu.edu.

‡ University of North Carolina.

§ North Carolina State University.

10.1021/jp8068514 CCC: $40.75
Published on Web 11/04/2008

multilayer islands at each of the critical points on the growth curve, and water contact angle goniometry to measure surface hydrophobicity as a function of oleic acid coverage. In analogy with similar growth patterns observed for vapor-deposited metals on oxide surfaces, we discuss a proposed mechanism for the observed surface morphologies in the context of our experimental results.

Experimental

Vapor Deposition. A home-built oven provided for precise temperature control for the vapor deposition studies. The oven consisted of a rectangular aluminum box (5 in. × 5 in. × 9 in.) with a hinged door. Holes were drilled into the oven walls through which cartridge heaters and a thermocouple were inserted. The oven was encased in 2-in.-thick, plain-faced, mineral wool insulation (McMaster-Carr), and wrapped in aluminum foil. A temperature controller maintained the oven temperature to within ±1 °C. Silicon wafers with an intrinsic oxide layer (silica) of ∼15 Å were cleaned by exposure to UV/O_3 in a commercial instrument and washed with distilled water. The substrate was placed across the top of a beaker containing oleic acid that had been preheated to the deposition temperature. An inverted beaker covered the sample. In the case of high humidity experiments, a dish of water was placed in the oven several hours before the experiments began, and the inverted beaker was omitted. For low humidity experiments, a beaker of Drierite was placed in the oven. Relative humidity was measured with a hygrometer to be 25% in the oven for experiments in the absence of the beaker of water or Drierite, 94% for the high-humidity studies, and 19% for the low-humidity studies.

Ellipsometry. An Auto EL null ellipsometer (Rudolph Research) provided output values of Ψ, which measures the ratio of the amplitude changes in s- and p-polarized light upon reflection from a surface; Δ, the change in phase between s- and p-polarized light; and d, thickness (assuming an index of refraction inputted by the user).[17] The excitation source was at $\lambda = 6328$ Å and incident on the surface at $\varphi = 70°$. The index of refraction (n_f) for oleic acid and silica is similar, ∼1.46. All measurements of oleic acid thickness were corrected for the intrinsic silica layer, which was measured prior to oleic acid deposition. In the thin film regime ($d < 50$ Å), Ψ varies only slightly, and the ellipsometric angle Δ contains information on the effective index of refraction and thickness of the film.[18] We utilized the form $\tan(\Delta - \Delta_0) = -C_\Delta d$ to analyze our data,[18] where Δ is the measured angle versus time, Δ_0 represents the phase shift due to reflection at the substrate (for silicon, ∼179°), and C_Δ contains the dependence on the indices of refraction of the film, substrate, and surroundings; the wavelength; and the angle of incidence. The film thickness is given by d. For our case of measurements in ambient ($n = 1$) conditions, a film with $n_f = 1.46$, and a silicon substrate with a complex index of refraction, $n_s - ik_s = 3.8816 - 0.01897i$, $C_\Delta = (4\pi/\lambda)[(\cos\varphi \sin^2\varphi)/\mu][(n_f^2 - 1)(1 - n_f^2\alpha)/n_f^2]$, where $\mu = \cos^2\varphi - \alpha + \alpha^2 \sin^2\varphi$, and $\alpha = (n_s^2 - k_s^2)/[(n_s^2 + k_s^2)]^2$.[19]

We utilized this analysis in two different ways. First, to give a general impression of surface coverage, we modeled the oleic acid coating as a continuous film, covering the native oxide. In this scheme, C_Δ is a constant, and Δ is linear in d. Thicknesses obtained from d before and after deposition were subtracted to obtain the effective thickness of the oleic acid layer. This approach is rigorously correct for a continuous film; however, for an islanded submonolayer, an effective medium model is more appropriate. Thus, a second, more detailed approach is to utilize the known thickness of the islands from AFM and to determine the effective index of refraction of this "film" consisting of some fraction of oleic acid and the remaining volume of air. In this case, d is set equal to the height of an island, and the equation for Δ is inverted to solve for n_f as a function of time, which will increase from an initial value of ∼1 (air) to $n_f = 1.65$ (oleic acid) if a complete monolayer of oleic acid is formed. This measured effective index-vs-time data is analyzed using an effective medium approach, which determines an effective index from two component indices and their relative fractions to obtain the fractional coverage of oleic acid at each time. Different effective medium models vary in their host medium: either one component is considered minor with the other serving as the host or both components are embedded in a host medium with a self-consistent effective index reflecting the current fractional distribution. We have chosen the latter Bruggeman effective medium model given by[17] $0 = f_A(n_A^2 - n_f^2)/(n_A^2 + 2n_f^2) + (1 - f_A)(n_B^2 - n_f^2)/(n_B^2 + 2n_f^2)$, for two components with differing indices (n_A and n_B), which is a useful approach when neither component is dominant. Essentially, this equation results from the Clausius−Mossotti formula, which relates the effective dielectric constant (n^2) to the various polarizabilities in the material, where each polarizability term is written in terms of the dielectric constant of that component material.[20] When utilizing an effective medium approach, the fused-silica layer is accounted for by subtracting the Δ values before and after deposition.

AFM Measurements. Measurements were taken with an Autoprobe M5 AFM (Thermomicroscopes). All images were taken using an aluminum-coated silicon cantilever with a radius of curvature of 10 nm (MikroMasch NCS15/ALBS) in non-contact mode. Typical scanning conditions are described in Garland et al.[16] Image backgrounds were flattened with AutoProbe Image software. A Visual Basic program was written to calculate the size distributions of the islands in the images.[16]

Contact Angle Goniometry. A droplet of water was pipetted onto the sample surface, and an image was collected with a digital camera located at a position perpendicular to the plane of the silica substrate. The angle between the surface and the droplet was measured with image analysis software. To account for the presence of islands on the surface, Cassie's equation[21] was utilized to analyze the water contact angle results, where $\cos\theta = f_a \cos\theta_a + f_b \cos\theta_b$, with θ the observed angle, $\theta_{a,b}$ the contact angles of oleic acid and silica, and $f_{a,b}$ the fractional coverages of oleic acid and silica, respectively.

Results and Analysis

Rate of Oleic Acid Growth on Silica. Figure 1 shows average thickness (d) obtained from ellipsometry measurements as a function of deposition time at oven temperatures of 60, 70, and 80 °C, assuming a uniform film with an index of refraction of 1.46 (see the Experimental section). Although we show later that the oleic acid does not coat the surface uniformly, we present the data in Figure 1 in units of film thickness (assuming an even coating) so as to provide an estimate of the volume of material on the surface. For short deposition times of up to a few minutes, the growth of oleic acid proceeds initially very fast and then levels off. From approximately 10 to 500 min, there appears to be very little additional growth. However, as the deposition time increases to thousands of minutes, the amount of material on the surface (here represented as an effective thickness) increases linearly with time. We label these three regions of growth I (rapid initial growth), II (slow intermediate growth), and III (fast growth at long times).

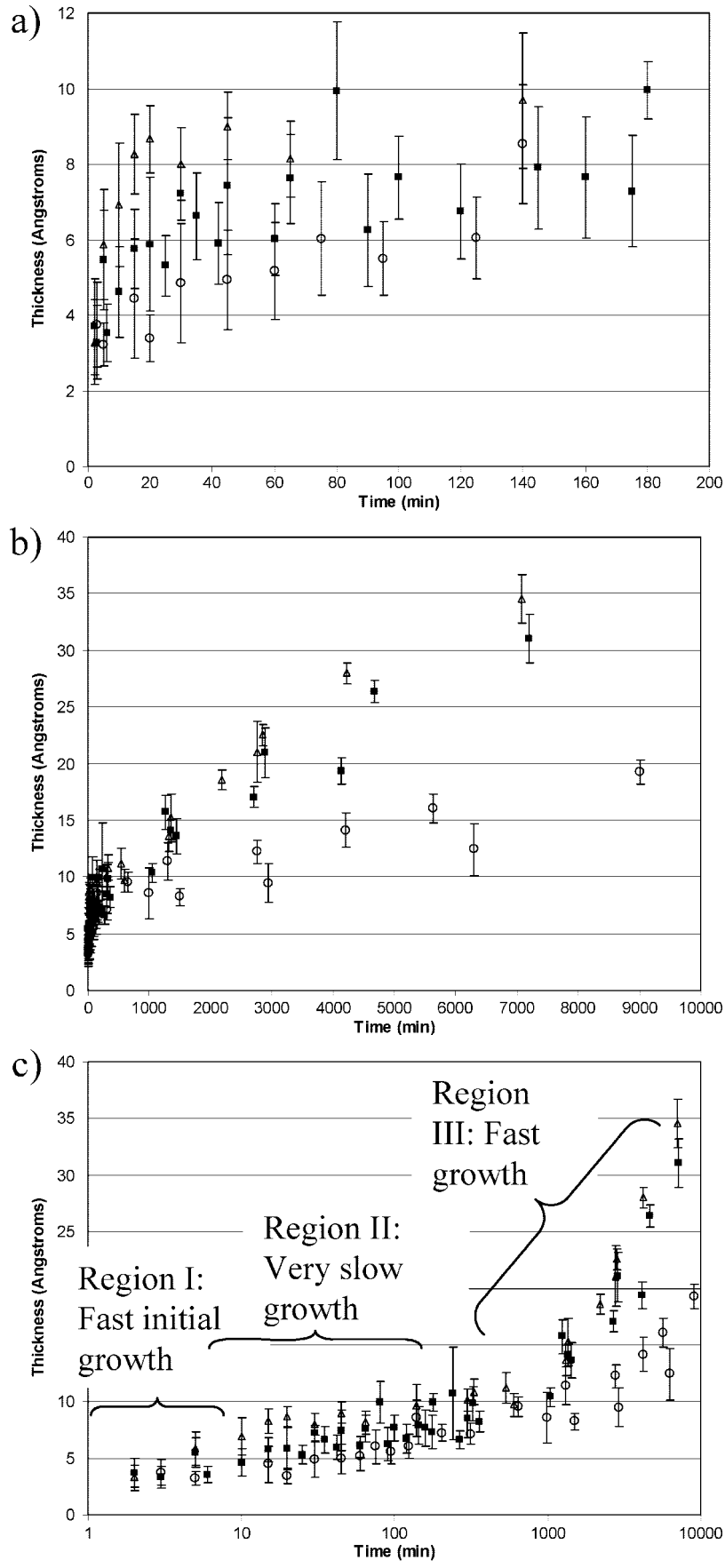

Figure 1. Ellipsometry measurements at 60 (○), 70 (■), and 80 °C (△) as a function of deposition time. The raw data obtained from ellipsometry were converted to an estimated, equivalent thickness of oleic acid, assuming an even coating on the surface. Panel a depicts the fast growth at short time scales, panel b shows the near-linear growth as a function of time at longer time scales, and panel c presents the data on a log scale so that the three regions of growth (I, II, and III) are clearly evident.

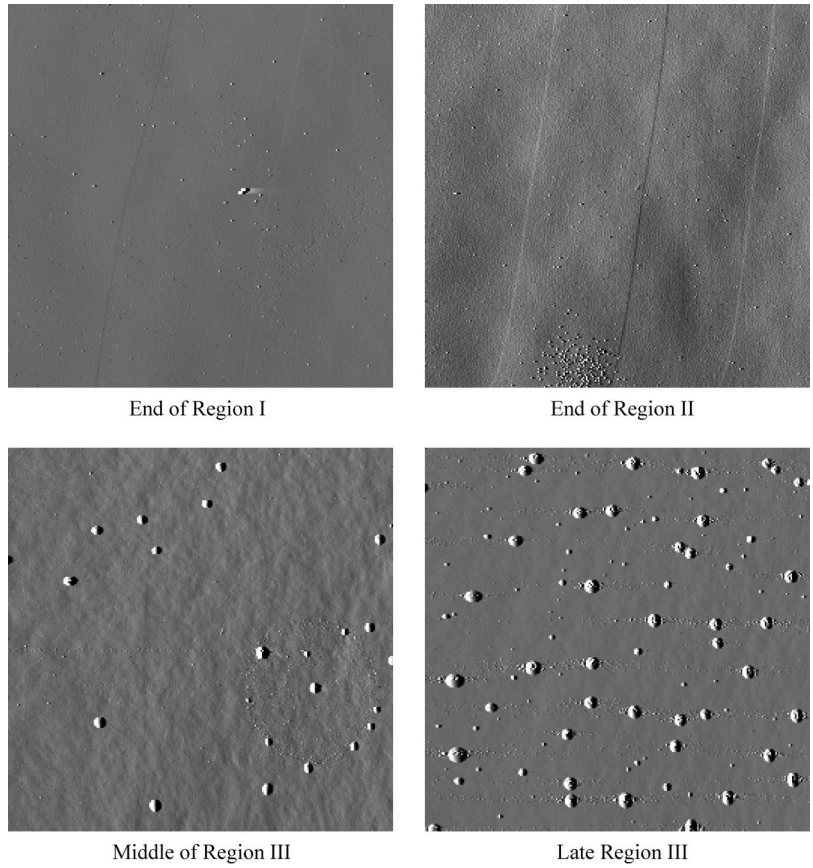

Figure 2. AFM images at different regions of growth for a deposition at 80 °C. All images are 40 μm × 40 μm.

As shown in Figure 1, the rate of deposition increases with increasing temperature. Because most of the initial fast growth occurs on timescales shorter than can be precisely accessed experimentally, we cannot compare the rates in region I at different deposition temperatures. For region III, the growth is linear in time for all temperature ranges. A simple model for this region of the deposition is that the thickness is proportional to the flux of molecules to the surface multiplied by a sticking coefficient. However, we find that such a model does not quantitatively describe our experimental results. The slope of growth is 0.0042 Å/s ($R^2 = 0.95$) at 80 °C, 0.0038 Å/s ($R^2 = 0.90$) at 70 °C, and 0.0016 Å/s ($R^2 = 0.82$) at 60 °C. The vapor pressure of oleic acid is 9×10^{-6} Torr at 60 °C, 3×10^{-5} Torr at 70 °C, and 1×10^{-4} Torr at 80 °C.[22] Thus, from 60 to 80 °C, the vapor pressure of oleic acid increases by an order of magnitude, but the rate of growth of oleic acid on the surface increases by only a factor of 2. If the rate of deposition depended only upon the collision rate multiplied by the sticking coefficient, the deposition rate would scale directly with vapor pressure. Therefore, our simple model is likely complicated by factors such as different sticking coefficients of oleic acid on silica and on adsorbed oleic acid and slow diffusion of oleic acid associated with the formation of multilayer islands (discussed below).

Morphology of Oleic Acid on Silica Surface. To better understand the physical processes underlying the three growth regions, AFM was used to observe the structure of the oleic acid on the surface. Figure 2 shows AFM images at key points on the growth curve of the 80 °C deposition from Figure 1. Throughout regions I and II, small islands of approximately 100 nm in diameter and 20−30 Å height are evident, which are consistent with a two-dimensional island of oleic acid, oriented perpendicular to the surface.[16] In the middle of region III, the number of smaller islands decreases, and larger multilayer islands appear. In late region III, most of the islands are significantly larger (1−2 μm diameter).

Figure 3 shows a histogram of island heights for a 40 μm × 40 μm region of each sample from Figure 2. The 100 nm diameter islands in regions I and II are all approximately 20−30 Å tall. As reported previously, we believe that these islands consist of oleic acid molecules oriented vertically in order to maximize interactions between the acid groups of the oleic acid with the hydroxyl groups of the silica surface.[16] The larger diameter islands in region III contain multiple layers of oleic acid. The histograms reveal that these islands are on the order of hundreds to thousands of Ås in height.

Taking this information into account, we further analyze the ellipsometry results presented above in order to determine areal coverage as a function of time, assuming islands of 25 Å in regions I and II (see experimental for methodology). These results are presented in Figure 4b and are compared to calculations from contact angle measurements, presented below. We were unable to perform a similar analysis in region III, since we could not assume a single island height (which is required for the analysis) because the multilayer islands varied in size in this region.

Wetting properties. Contact angle goniometry measured surface wetting properties in order to distinguish between a Stranski-Krastanov growth mechanism, in which oleic acid forms a thin continuous film on the surface followed by the formation of islands, and a Volmer−Weber growth mechanism, in which islands form directly on top of the bare surface.[23,24] The water contact angle as a function of deposition time is shown in Figure 4a and compared to the thickness measured with ellipsometry. If the islands formed on top of a layer of upright oleic acid, the water contact angle would be expected

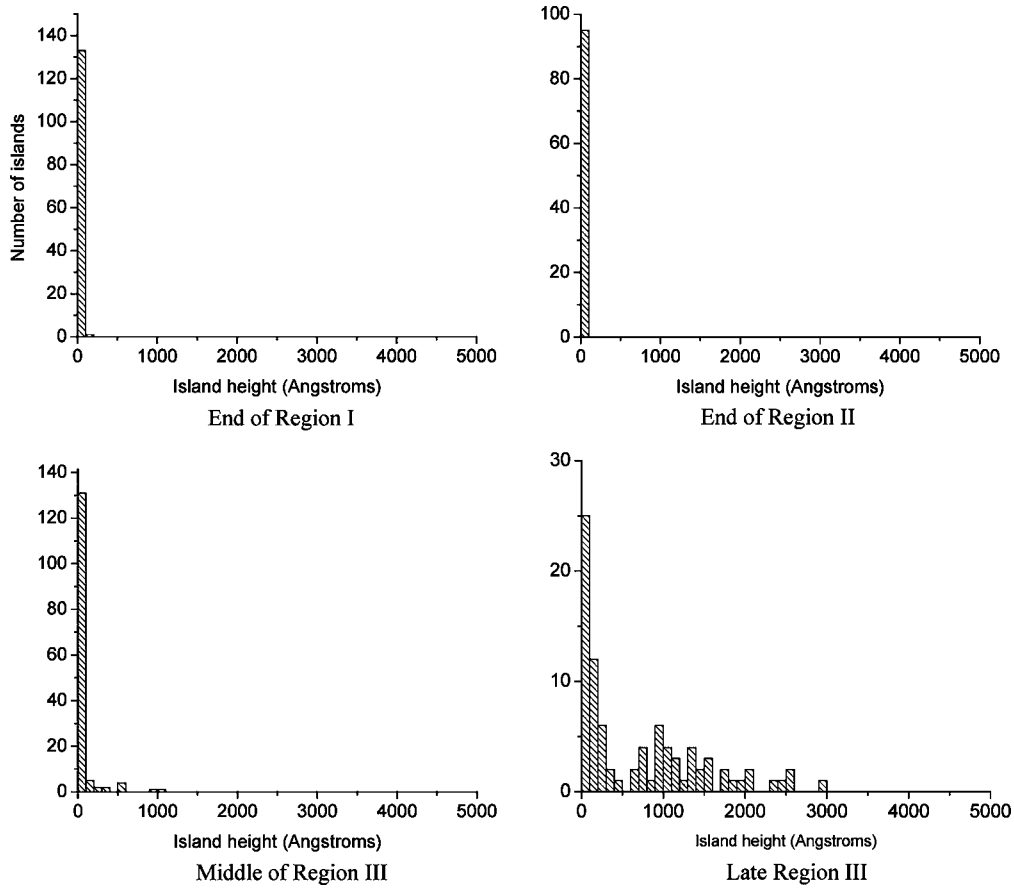

Figure 3. Histograms of island heights for each of the images in Figure 2.

to level off once such a monolayer was formed. In fact, the contact angle increases with deposition time, indicating that the surface is becoming more hydrophilic.

Cassie's equation for an islanded film was utilized to further analyze the contact angle results in regions I and II and determine an effective coverage (Figure 4b), assuming water contact angles of 0° and 120° for silica and oleic acid, respectively. The contact angle of oleic acid depends strongly on its orientation with respect to the surface (i.e., the portion of the molecule accessible to the water droplet). The value of 120° is consistent with upright molecules with the carboxylic acid nearest to the silica surface.[25] If oleic acid molecules first coated the surface, we expect the estimates from Cassie's equation to overestimate the coverage, as the contact angle of the open space (covered with oleic acid) would have a higher contact angle than the neat silica surface, as assumed in our calculation. The coverage obtained from Cassie's equation agrees well with the results from the ellipsometry measurements except at low coverages. In this region, the results indicate a contact angle in the island regions less than 120°, which could indicate some orientational disorder of the oleic acid. Therefore, within our experimental error, the contact angle results suggest that a bare silica surface remains exposed under the oleic acid islands throughout the deposition, characteristic of the Volmer−Weber growth model. Thus, even when the surface is covered with large islands containing a mass of oleic acid equivalent to many monolayers of coverage, a significant fraction of the silica surface remains exposed to the air. Under atmospheric conditions, this exposed silica surface may be available to interact with other species.

Mechanism of Island Growth. The results presented above delineate a growth mechanism for vapor deposition of oleic acid at low humidities onto fused silica that begins with formation of two-dimensional islands, one molecule thick, and transitions at a low coverage (~10%) to three-dimensional island growth. At no point during this process is a uniform layer observable, and throughout the ~5 days process, a significant fraction of the fused silica is apparently unwetted by oleic acid. We now discuss the possible underlying mechanism associated with this observed growth process.

As discussed in the introduction, only a few reports have examined the mechanism of vapor deposited film growth of organics on oxide surfaces involving island formation. Furthermore, a Volmer−Weber growth mechanism usually involves three-dimensional island formation at the onset of growth, rather than the transition which we observe from two-dimensional islands to three-dimensional islands.[26] A similar growth kinetic curve as that in our study, in which islands are initially formed quickly and then growth levels off before increasing linearly, has been observed for the solution-phase deposition of octadecylphosphonic acid on mica.[27] However, in that study, only monolayer-high islands were observed.

Since we were unable to find any reports of organic species on oxides with a growth mechanism analogous to our observations of oleic acid on silica, we expanded our search to a broader range of systems. We found a similar growth pattern for the case of vapor deposition of metal atoms on oxide surfaces, modeled by Campbell and Ludiviksson.[28] In this model, it is assumed that atoms adsorb and readily diffuse, be it on the bare substrate or over existing adsorbates. Islands nucleate when two atoms collide on the surface. The key features of the model are 1) a potential well near the edge of each island, which reflects the strong atom-atom interaction of the metal and forces island growth, and 2) a small difference between the energy of an atom

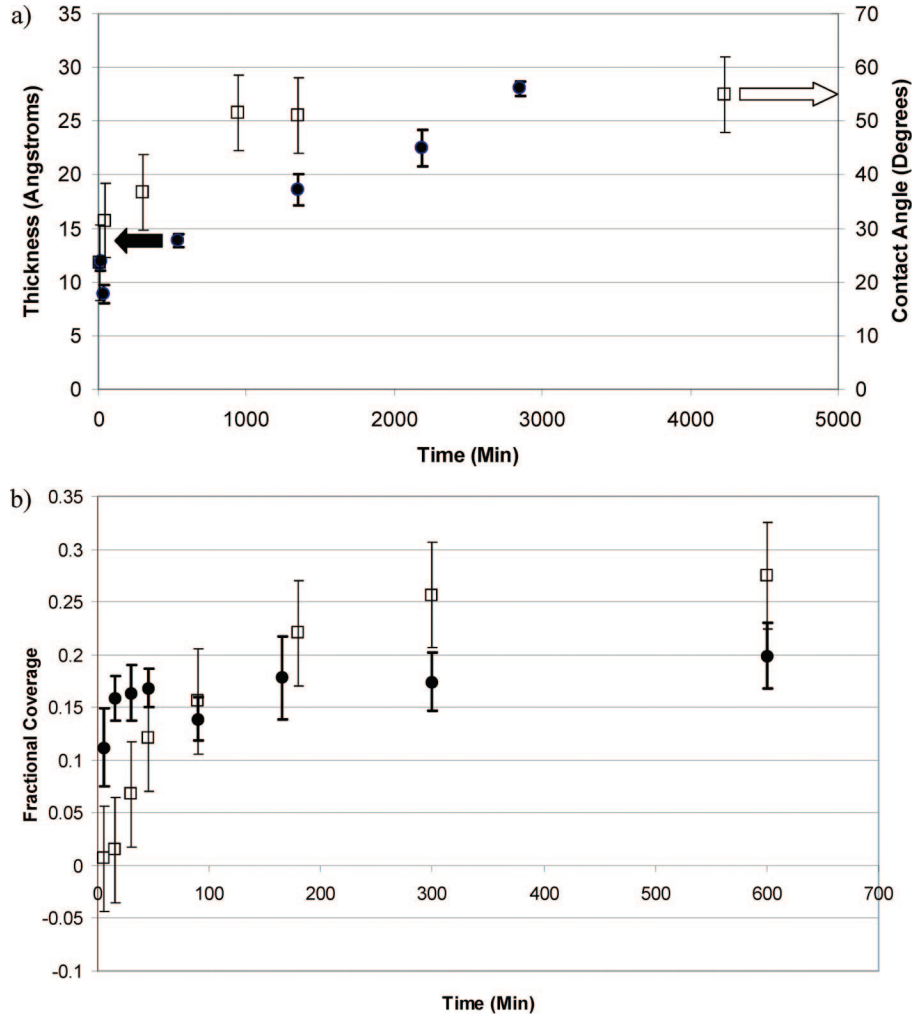

Figure 4. a. Dependence of contact angle on deposition time for 80 °C samples compared with thickness estimates (continuous model) over three deposition regions. b. Fractional surface coverage calculated from ellipsometry (●, effective medium model) and contact angle measurements using Cassie's equation (□) for data from regions I and II.

adsorbed on an island and one adsorbed on the surface. At low coverage, an adsorbed atom initially landing on the surface will diffuse until it encounters another atom, forming a nucleation site, or an island, where it becomes trapped. An atom landing on an existing island will diffuse to the edge of the island and increase the island's lateral size. As island size increases, the surface area covered by islands increases, making it more likely that an adsorbate will land on an existing island, and increasing the time needed to diffuse to the island edge. Thus, at some critical coverage (dependent on the parameters of the system), it becomes more likely for two atoms to collide on an island, rather than diffusing to the edges. For gold atoms on TiO_2 (150−300 K), the critical coverage is dependent on temperature but occurs at approximately 10%.[26] In this case, the atoms nucleate a second layer, with a potential well at its edge deeper than that of the monolayer island, due to the difference in environment of an atom surrounded on two sides with other atoms, as opposed to a single atom-atom contact at the edge of the monolayer island. As the size of the second layer approaches that of the first, atoms at the edge of the monolayer reduce their energy by "stepping up" and joining the second layer. Similar processes occur for subsequent layers until bulk-like droplets are formed. These authors point out that three-dimensional growth is energetically preferred; however, kinetic effects trap the system in two-dimensional islands early in the growth process. It is common for film deposition to initially produce surface structures that are far from equilibrium but trapped in an energy well.[29]

We consider the application of this model to the oleic acid-fused silica system. It is reasonable that adsorbate oleic acid molecules are quite mobile on the silica surface, particularly with small amounts of water present. (The possibility that the initial islands were formed by oleic acid vapor phase nanodroplets, rather than oleic acid monomers, was discarded because nanodroplets can only be formed under conditions of supersaturated vapor, which were not present for our experiments.[30]) Such mobility seems likely due to the quick formation of the small (100 nm diameter) islands. Oleic acid molecules have significant Van der Waals interactions, which would encourage island growth due to a potential well at the perimeter of existing islands. In the oleic acid case, the growth of the larger multilayer islands occurs on a much longer time scale than the initial growth of the smaller islands. When vapor phase oleic acid deposits directly on top of an existing oleic acid island, the interaction energy will be strongly dependent on molecule orientation and could be greater or less than the strong hydrogen bonding it can attain with the silica surface. This is a significant difference from the atomic system, and may slow dynamics.

Ripening. The AFM images show that large islands form when unlimited oleic acid is available from the vapor phase. To test whether large islands are preferred thermodynamically at low coverage, we prepared a sample containing predominantly

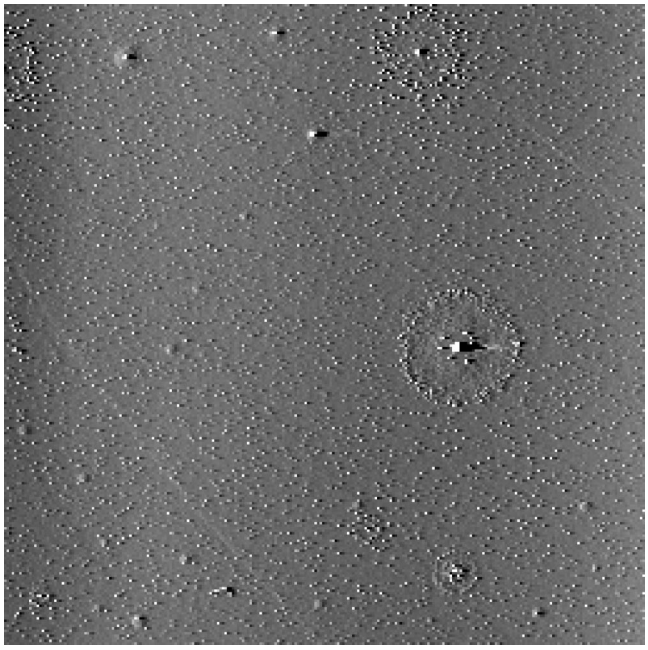

Figure 5. Sample from end of region II after annealing for 7 days at 80 °C. Image is 40 μm × 40 μm.

small islands (end of region II). Then, we annealed this sample in the oven at 70 °C for 7 days with no additional oleic acid present. Ellipsometry measurements remained constant throughout the entire annealing time, indicating that most of the oleic acid remained on the surface. However, the surface contained significantly larger islands after annealing, indicating that the larger islands are thermodynamically favored over the smaller islands (Figure 5).

The transformation of small islands into larger islands is called ripening and may occur through either the Smolouchowski or Ostwald mechanism.[31] In the Smolouchowski mechanism, small islands migrate, and merge into larger islands when they collide with each other, while in the Ostwald mechanism, individual molecules preferentially evaporate from smaller islands (due to their higher vapor pressure) and may recondense on larger islands. Since we cannot follow a specific region of the surface over the course of the deposition with AFM, we cannot differentiate between the mechanisms. However, multiple images of the surface at the end of region II, as well as the annealed sample (Figure 5), show small islands that are grouped closely together, sometimes in a circular formation. Such images may be evidence for a Smolouchowski mechanism.

Effect of Humidity. Models have shown that water preferentially interacts with −OH groups on a silica surface.[32,33] Thus, in the presence of high relative humidity, water may compete with the oleic acid for adsorption sites on the silica. To test whether the presence of large amounts of water vapor would alter the dynamics of oleic acid adsorption on silica, we performed depositions under both high and low relative humidities.

Depositions of oleic acid at 94 and 19% relative humidities produced similar ellipsometry curves at all times (Figure 6). The oleic acid in the oven decomposed more quickly in the presence of water vapor, as indicated by a yellow coloring of the oleic acid; therefore, we were unable to experimentally access time scales of more than a few days. Unlike the low-humidity AFM images, the AFM images for the high-humidity samples showed no evidence of island formation (Figure 7). The contact angle of water on the high-humidity sample after 23 h of deposition was 42°. Since the contact angle of water on silica is close to 0°, this contact angle measurement confirmed that there is oleic acid on the surface. However, rather than forming islands, at high relative humidity oleic acid appears to spread out on the surface of the silica.

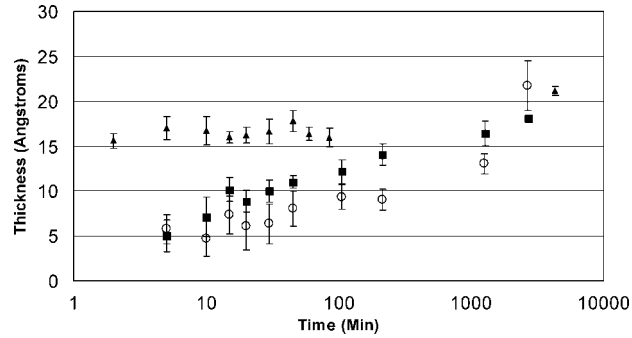

Figure 6. Ellipsometry results for high relative humidity (94%) sample (■), low relative humidity (19%) sample (○), and high-humidity sample pre-exposed to water vapor (▲). The values of Δ obtained from ellipsometry were converted to an estimated, equivalent thickness of oleic acid, assuming an even coating on the surface for ease of comparison between the three systems. The initial points for the pre-exposed high-humidity sample are due to water on the silica surface.

We also investigated the effect of first placing the silica sample in the oven with water for several hours and then adding oleic acid vapor. Goodman et al.[34] found that at a relative humidity of 94%, several monolayers of water molecules deposit on a silica surface. After being exposed to 94% humidity for 12 h, ellipsometry measurements indicated growth (in addition to the native oxide), which we attribute to water on the surface of the silica. When these samples were subsequently exposed to oleic acid vapor, there was no increase in the thickness as measured by ellipsometry on short time scales, but the sample behaved similarly to the other samples at long time scales (Figure 6). We believe the difference in the short time scale data can be attributed to the presence of water on the surface blocking adsorption sites from the vapor phase oleic acid molecules. As with the previous high humidity experiment, AFM images did not indicate the presence of island formation.

The results of these high-humidity studies show that the presence of a high concentration of water vapor causes the oleic acid to wet the surface, spreading evenly rather than forming discrete islands. Such a result is not unexpected, as a drop of water placed on top of liquid oleic acid will spread evenly over (wet) the surface. Thus, the morphology of oleic acid on a silica surface is dependent on relative humidity due the different wetting properties of oleic acid on water or the native silica surface.

Summary and Conclusions

We have found that the adsorption of oleic acid onto silica at low humidities occurs via two processes. The first process occurs on the time scale of several minutes and results in monolayer high oleic acid islands that are relatively uniform in size. The second adsorption process occurs on a time scale of hours to days and results in multilayer islands that increase in size as a function of deposition time. Ripening and further deposition of the oleic acid from the gas phase ultimately move the system toward the thermodynamically preferred state of multilayer oleic acid islands.

We further find that the nature of adsorption of oleic acid on silica is highly sensitive to relative humidity. Oleic acid molecules do not form islands on silica surfaces at high relative humidity; instead, the oleic acid spreads out on the silica surface. The range

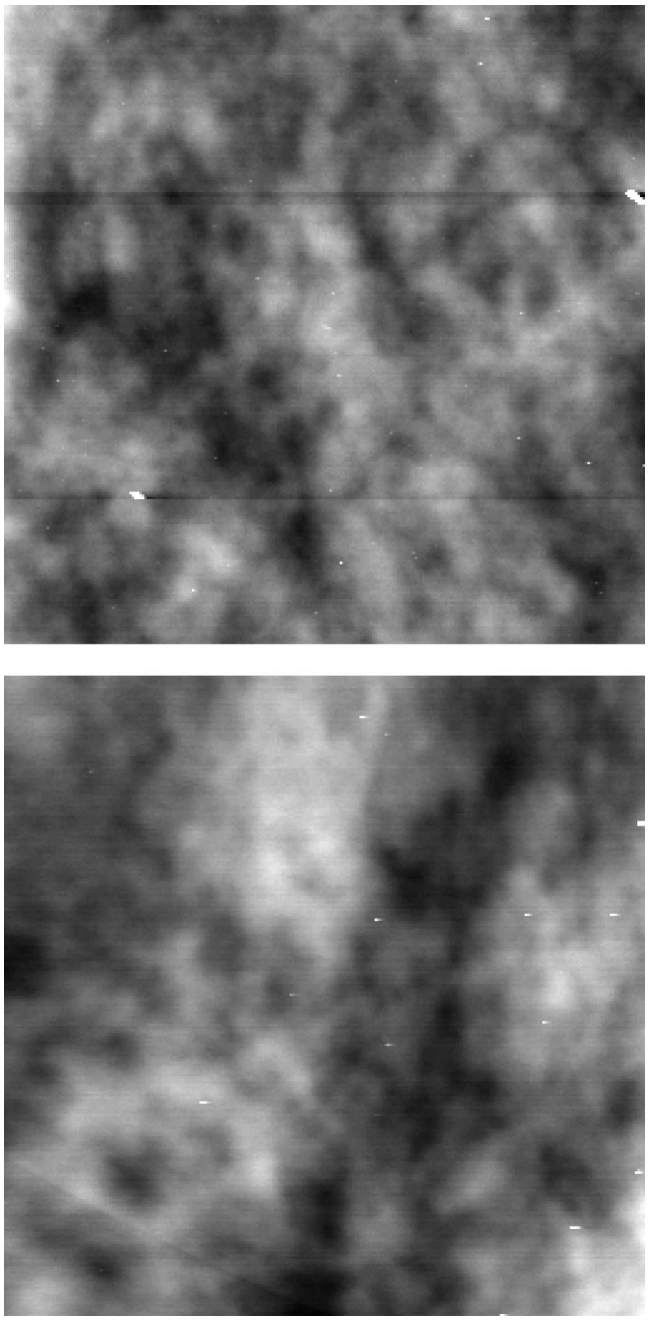

Figure 7. AFM images of silica exposed to 94% humidity at 80 °C for 24 h (top) and silica exposed to 94% humidity and oleic acid at 80 °C for 48 h (bottom). Images are 40 μm × 40 μm. Area analyses indicate a rms roughness of 6.7 Å for both images.

of humidities used in our experiments (20−94%) is representative of conditions that may be found in the atmosphere, and so the morphology of organic species deposited on environmental surfaces may be highly dependent on the local humidity.

The morphology of adsorbate molecules on surfaces can impact a number of surface properties. One example of such an effect is hydrophobicity, which we directly measured using contact angle goniometry. As expected, we found that the hydrophobicity of the surface increased as a larger fraction of the silica surface was blocked by oleic acid. However, even at high coverages (equivalent to several monolayers), some of the silica surface is likely exposed under lower humidity conditions due to the presence of oleic acid islands. In addition to direct effects on hydrophobicity, the morphology of the oleic acid is expected to indirectly affect hydrophobicity for atmospherically relevant situations. Large islands would inhibit the oxidation of oleic acid by ozone, which is known to occur via a surface mechanism. The oxidized products of oleic acid serve as better cloud condensation nuclei, and so large islands would decrease the rate of transformation from a hydrophobic to a more hydrophilic surface.[35,36] Similar direct and indirect effects on hydrophobicity, reactivity, and radiative properties are expected to be influenced by the surface morphology of oleic acid and other organic molecules deposited onto inorganic substrates.

Acknowledgment. We thank Dr. Elias P. Rosen for helpful discussions. Funding from a NSF grant to the University of North Carolina at Chapel Hill is gratefully acknowledged.

References and Notes

(1) Smoydzin, L.; von Glasow, R. *Atmos. Chem. Phys.* **2007**, *7*, 5555.
(2) Xiong, J. Q.; Zhong, M. H.; Fang, C. P.; Chen, L. C.; Lippmann, M. *Environ. Sci. Technol.* **1998**, *32*, 3536.
(3) Schwarz, J. P.; Spackman, J. R.; Fahey, D. W.; Gao, R. S.; Lohmann, U.; Stier, P.; Watts, L. A.; Thomson, D. S.; Lack, D. A.; Pfister, L.; Mahoney, M. J.; Baumgardner, D.; Wilson, J. C.; Reeves, J. M. *J. Geophys. Res., [Atmos.]* **2008**, 113.
(4) Riziq, A. A.; Trainic, M.; Erlick, C.; Segre, E.; Rudich, Y. *Atmos. Chem. Phys.* **2008**, *8*, 1823.
(5) Saizjimenez, C. *Atmos. Environ., Part B* **1993**, *27*, 77.
(6) Yang, X.; Chen, Q.; Zhang, J. S.; An, Y.; Zeng, J.; Shaw, C. Y. *Atmos. Environ.* **2001**, *35*, 1291.
(7) Vacha, R.; Cwiklik, L.; Rezac, J.; Hobza, P.; Jungwirth, P.; Valsaraj, K.; Bahr, S.; Kempter, V. *J. Phys. Chem. A* **2008**, *112*, 4942.
(8) Cosman, L. M.; Knopf, D. A.; Bertram, A. K. *J. Phys. Chem. A* **2008**, *112*, 2386.
(9) Ellison, G. B.; Tuck, A. F.; Vaida, V. *J. Geophys. Res., [Atmos.]* **1999**, *104*, 11633.
(10) Rosen, E. P.; Garland, E. R.; Baer, T. *J. Phys. Chem. A* **2008**, *112*, 10315.
(11) Ong, B. S.; Wu, Y. L.; Li, Y. N.; Liu, P.; Pan, H. L. *Chem.—Eur. J.* **2008**, *14*, 4766.
(12) Kubono, A.; Yuasa, N.; Shao, H. L.; Umemoto, S.; Okui, N. *Appl. Surf. Sci.* **2002**, *193*, 195.
(13) Mayer, A. C.; Ruiz, R.; Zhou, H.; Headrick, R. L.; Kazimirov, A.; Malliaras, G. G. *Phys. Rev. B* **2006**, 73.
(14) Park, Y. D.; Lim, J. A.; Lee, H. S.; Cho, K. *Mater. Today* **2007**, *10*, 46.
(15) Rudich, Y.; Donahue, N. M.; Mentel, T. F. *Annu. Rev. Phys. Chem.* **2007**, *58*, 321.
(16) Garland, E. R.; Rosen, E. P.; Clarke, L. I.; Baer, T. *Phys. Chem. Chem. Phys.* **2008**, *10*, 3156.
(17) Tompkins, H. G., Iene, E. A., Eds. *Handbook of Ellipsometry*; William Andrew Pub. Norwich, NY, 2005.
(18) Saxena, A. N. *J. Opt. Soc. Am.* **1965**, *55*, 1061.
(19) Palik, E. D.; Ghosh, G. *Handbook of Optical Constants of Solids*; Academic Press: San Diego, 1998.
(20) Aspnes, D. E. *Thin Solid Films* **1982**, *89*, 249.
(21) Cassie, A. B. D. *Discuss. Faraday Soc.* **1948**, *3*, 11.
(22) Tang, I. N.; Munkelwitz, H. R. *J. Colloid Interface Sci.* **1991**, *141*, 109.
(23) Somorjai, G. A. *Introduction to Surface Chemistry and Catalysis*; John Wiley & Sons, New York, 1994.
(24) Hudej, R.; Bratina, G.; Onellion, M. *Thin Solid Films* **2006**, *515*, 1424.
(25) Wang, C. Y.; Zhao, X.; Zhao, J. Z.; Liu, Y. H.; Sheng, Y.; Wang, Z. C. *Appl. Surf. Sci.* **2007**, *253*, 4768.
(26) Parker, S. C.; Grant, A. W.; Bondzie, V. A.; Campbell, C. T. *Surf. Sci.* **1999**, *441*, 10.
(27) Doudevski, I.; Hayes, W. A.; Schwartz, D. K. *Phys. Rev. Lett.* **1998**, *81*, 4927.
(28) Campbell, C. T.; Ludviksson, A. *J. Vac. Sc. Technol., A* **1994**, *12*, 1825.
(29) Morgenstern, K. *Phys. Status Solidi B* **2005**, *242*, 773.
(30) McDonald, J. E. *Am. J. Phys.* **1962**, *30*, 870.
(31) Lo, A.; Skodje, R. T. *J. Chem. Phys.* **2000**, *112*, 1966.
(32) Ma, Y. C.; Foster, A. S.; Nieminen, R. M. *J. Chem. Phys.* **2005**, 122.
(33) Rimola, A.; Ugliengo, P. *J. Chem. Phys.* **2008**, 128.
(34) Goodman, A. L.; Bernard, E. T.; Grassian, V. H. *J. Phys. Chem. A* **2001**, *105*, 6443.
(35) Asad, A.; Mmereki, B. T.; Donaldson, D. J. *Atmos. Chem. Phys.* **2004**, *4*, 2083.
(36) Broekhuizen, K. E.; Thornberry, T.; Kumar, P. P.; Abbatt, J. P. D. *J. Geophys. Res., [Atmos.]* **2004**, 109.

JP8068514